Graphical Abstract

Odorant molecular feature mining by diverse deep neural networks for prediction of odor perception categories

Liang Shang,Chuanjun Liu,Fengzhen Tang,Bin Chen,Lianqing Liu,Kenshi Hayashi

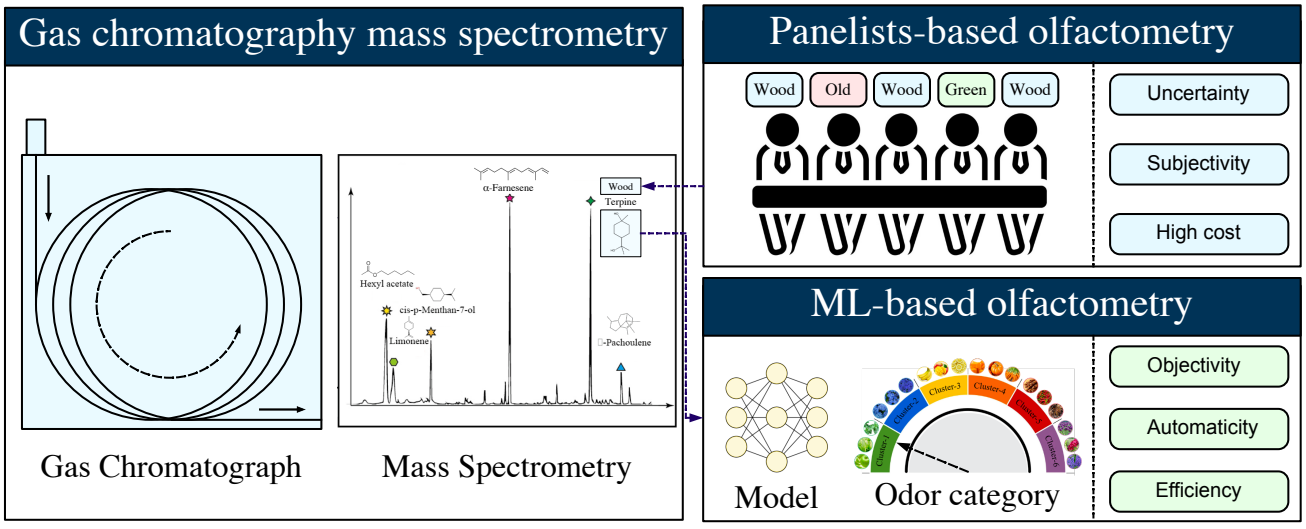

Highlights

Odorant molecular feature mining by diverse deep neural networks for prediction of odor perception categories

Liang Shang,Chuanjun Liu,Fengzhen Tang,Bin Chen,Lianqing Liu,Kenshi Hayashi

- Different deep neural networks were used to predict categorized odor descriptors.
- End-to-end-based representation learning was performed for molecular feature extraction.
- Molecular graphs with pre-training of convolution neural networks was most accurate.

Odorant molecular feature mining by diverse deep neural networks for prediction of odor perception categories

Liang Shang[a,b,*], Chuanjun Liu[c,d], Fengzhen Tang[a,b,*], Bin Chen[e], Lianqing Liu[a,b] and Kenshi Hayashi[c]

[a]State Key Laboratory of Robotics, Shenyang Institute of Automation, Chinese Academy of Sciences, Shenyang, 110016, China
[b]Institute for Robotics and Intelligent Manufacturing, Chinese Academy of Sciences, Shenyang, 110016, China
[c]Department of Electronics, Graduate School of Information Science and Electrical Engineering, Kyushu University, Fukuoka, 819-0395, Japan
[d]Research Laboratory, U.S.E. Co., Ltd., Tokyo, 150-0013, Japan
[e]Chongqing Key Laboratory of Non-linear Circuit and Intelligent Information Processing, College of Electronic and Information Engineering, Southwest University, Chongqing, 400715, China

ARTICLE INFO

Keywords:
Odor sensory category
Structure odor relationship
Odorant molecules structure features extraction
Machine learning
Recognition and classification

ABSTRACT

The prediction of structure-odor-relationship (SOR) by deep neural networks (DNN) via the structural features of odorants has attracted great attention during the past decade. Due to the limited knowledge on binding mechanism between odorant molecules and olfactory receptors, however, it is not sure what kind of structural features play the most important role in smell recognition. In this work, diverse deep neural networks, including molecular parameters neural network (MPNN), molecular graphic convolution neural network (MG-CNN), molecular graph transformer neural network (MGTNN) and atom interaction neural network (AINN), were used to extract the structure features of odorant molecules and to predict the categorized odor perception. We optimized all of the models via parameter tuning, and evaluated and compared their performance using a database containing 2849 odorants and their corresponding odor sensory category labels. The experimental results demonstrated that an MG-CNN (pre-trainedResNet) combined with a multi-label DNN classifier produced the best results, with an area under the receiver operating characteristic curve and F1 score of 0.877±0.028 and 0.726±0.028, respectively. This is the first systematic study for molecular structure features extracted by different deep neural network and their predictive effect for SOR. We believe that these insights regarding the use of DNN-based odorant molecular feature extraction for odor sensory identification will be useful for introducing biologically interpretable artificial intelligence into olfactometry, and thus contribute to our understanding of the mechanisms underlying human olfaction.

1. Introduction

Identifying the interactions between odorants and sensory descriptions is important for the discovery and analysis of volatile compounds. To obtain the sensory information of odor, gas chromatography/olfactometry (GC/O) has been widely applied as a powerful odor analytic strategy in various research areas, such as agriculture, food, and environmental science [1–3]. Although GC/O can be used to attain accurate sensory and chemical characteristics of odorants, this approach is expensive and time-consuming, which can limit its application. The main expense associated with GC/O is the cost of hiring and training panelists to characterize the sensory qualities of odorants using their sense of smell. In addition, the sensory assessment of human panelists is personally dependent, which inevitably leads to subjectivity and inconsistency into the evaluation results.

Research on the response patterns of neurons in the olfactory bulbs (OB) has illuminated the mechanisms underlying biological olfaction [4–6]. However, many questions remain, such as why these molecules smell different from one another and why we link smell feelings with certain semantic descriptors, known as odor descriptors (ODs). These questions may be answered by examining structure odor relationships (SORs), the development of which presents a difficult and interesting challenge [7–9]. During recent years, many researches have been conducted to predict odor perception of odorants using vairous parameters, such as electronic or physicochemical characteristics [10, 11], mass spectrometry (MS) [12, 13], and social network interactions [14]. Additionally, novel methods, such as odor-based social networks [15–17], machine learning (ML) [18–20], deep neural network (DNN) models [21–24], and semantic-based approaches [25] have been developed to calibrate models that express the relationships between odorants and ODs. These studies have demonstrated the possibility to use data-driven approaches to solve the SOR problems. In line with this trend, we have proposed a concept of ML-based GC/MS olfactometry in which the sensory evaluation of panelists is expected to be replaced by machine learning prediction models [26].

In the ML-based GC/O system, the molecular information obtained by MS analysis of the individual GC peaks is transfered into physicochemical parameters by molecular calculation software (DRAGON). By building models appropriately, the ODs of the odorants can be predicted with high accuracy form their physicochemical parameters. The

*Corresponding author
shangliang0225@gmail.com (L. Shang); tangfengzhen@sia.cn (F. Tang)
ORCID(s): 0000-0001-8369-3049 (L. Shang); 0000-0002-7232-2573 (C. Liu); 0000-0002-4654-9440 (F. Tang); 0000-0002-3722-4740 (B. Chen); 0000-0002-2271-5870 (L. Liu); 0000-0001-8679-4953 (K. Hayashi)

ML-based GC/O is a concept-of-proof study and there are many problems to be solved before its practical application. For example, in terms of the sample size, only limited ODs with high frequency of occurrence are targeted in our models. In reality, it has been reported that over 500 ODs are used for odor evaluation [27]. Therefore, many ODs, especially for those rare ODs are not considered by the models. In oder to solve this issue, we have recently proposed a categorization approach based on the semantic analysis of ODs, which make the model can cover the prediction of several hundreds of ODs [28]. Another remaining problem is that the model prediction is based on physicochemical parameters of odorants. The recent development of computational chemistry and ML make it possible to obtain various molecular structure information [29]. Unlike traditional methods, DNNs can directly learn latent presentations from molecular structures, such as atom types and their positions, via back-propagation [30]. Moreover, an end-to-end strategy has been proposed as an effective nonlinear modeling method for learning molecular presentation in many fields, such as quantum chemical properties prediction, and compound-protein interaction identification [31]. However, since detailed binding mechanism between the odorants and olfactory receptors is still not fully understood, which molecular features play the most important role in olfactory perception has not been cleared.

The purpose of this study is dedicated to molecular feature mining by diverse DNNs for prediction of odor perception categories. Please note that our work is not to propose some novel classification frameworks, but using multi-type of feature extractors to understand the relationship between the structure features of odorants and odor perception categories. A schematic of the data processing and modeling procedures is illustrated in Fig. 1. We used molecular structures, including 2D molecular images and atom spatial locations, to predict odor sensory categories. For minding useful information from molecular structures, some molecular structural feature extraction methods were empoyed and their results were compared and discussed. Specifically, we used a molecular graphic convolution neural network (MG-CNN) and molecular graph transformer neural network (MGTNN) to extract features from representations of molecular structure, such as molecular structure images and topology graphs. Moreover, we used atom interaction neural networks (AINNs) to generate features from the spatial structures of atoms. To overcome limitations related to insufficient samples, we also considered pre-trained models, such as pre-trained CNNs and MGTNNs. We compared the feasibility of SOR prediction via molecular fingerprints, molecular parameters, and molecular feature extraction based on MG-CNN, MGTNN, and AINN. We achieved the highest performance by applying molecular features extracted via a pre-trained MG-CNN combined with a mulit-label learning model (area under the ROC curve: 0.877±0.028 and F1 score: 0.726±0.028). Thus, the proposed odor sensory category identification model is a feasible option for developing artificial intelligence (AI)-based GC/O. Although it would be still a challenge to replace human assessors by ML models perfectly, the proposed method could provide references for assessors to increase the efficiency for odor analysis. Therefore, the limitation of odor memory would be breaked through by the odor perception categories recommended by the proposed method.

2. Materials and methods

2.1. Data collection and preparation

To create an odor category prediction model, we collected an extensive dataset containing 2849 odorants. We used information from publicly available databases such as the Odor Map database [32], Flavors and Fragrances database (Sigma-Aldrich) [33], and the Good Scents database [34]. As illustrated in Fig. 1, we collected and prepared 5 types molecular descriptors, including molecular parameters, molecular fingerprints, molecular graphs, simplified molecular input line entry system (SMILES), and atom coordinates. Specifically, we used SMILES and RDKit Software (ver. 2021.03.1) [35, 36] to collect normalized molecular parameters (1826, detailed information can be found at [37]), molecular fingerprints (binary, 2048 bits), and 2D molecular graphs (RGB, 300×300 pixels). We used RDKit to obtain the 2D and 3D atom coordinates of the odorants, which we used to train the model regarding the atomic interactions between odorant structures and their odor sensory categories. In total, 256 ODs were clustered into 20 categories using a co-occurrence Bayesian embedding method. More detailed information regarding the cleaning and categorization of ODs can be found in Table S1 [28]. Data were processed and analyzed using Python (ver. 3.9.0) and R (ver. 4.1.1). Because the diverse molecular representations of odorants, we need to employ various of feature extraction technologies to obtain embeddings for model calibration.

2.2. Model calibration

The calibration and validation process for the odor category model is shown in Fig. 1. First, all samples were divided via random splitting into training and test sets with a 4:1 ratio, and the reported results are averaged over 50 repetitions. Afterward, we employed molecular parameters, molecular fingerprints, molecular graphic features, molecular graph transformers, and atomic interaction embedding to extract the molecular features of the odorants (Fig. 2). We used a DNN approach to develop a multi-label odor category learning model (the output size was 20) based on the aforementioned molecular information. The cost function $\mathcal{L}(\mathbf{\Theta})$ of the DNN multi-label classifier was calculated by summing the binary cross-entropy of each class, which was defined as follows:

$$\mathcal{L}(\mathbf{\Theta}) = \frac{1}{N}\sum_{i=1}^{N}\sum_{j=1}^{M} y_{i,j} \times \log(\hat{y}_{i,j}) + (1 - y_{i,j}) \times \log(1 - \hat{y}_{i,j}) \tag{1}$$

where $\boldsymbol{\Theta}$ indicates the parameter set of the model, N indicates the sample number in the training set, and M indicates the number of odor categories, set as 20 in the present study. $y_{i,j}$ and $\hat{y}_{i,j}$ are the ground truth and prediction label for category j of sample i, respectively. By minimizing the cost function based on the stochastic steepest gradient descent algorithm, parameters from the DNN could be learned and updated. For each DNN method, the number of hidden layers and nodes was selected from 1 to 8 layers and {16, 32, 64, 128, 256, 512, 1024, 2048} nodes, respectively. Network parameters, including the dropout ratio, learning rate, and training epoch, were set as 0.1, 1×10^{-4}, and 200, respectively. The optimal models were determined according to their areas under the ROC curve (AUC) and F1 scores based on precision and recall, simultaneously. Both qualitative and quantitative data analyses were performed.

Because molecular graphs, molecular SMILES sequences, and atom coordinates are not tabular data, they cannot be used as classifier inputs directly. Therefore, diverse feature extraction methods were firstly employed to convert those unstructured data to tabular features. Specifically, pre-trained CNNs, sequence transformer, and atomic interaction embedding were utilized for moelcular graphs, SMILES sequences, and atom coordinates features extraction, respectively. Detail information of above-mentioned strategies were summarized as fllows.

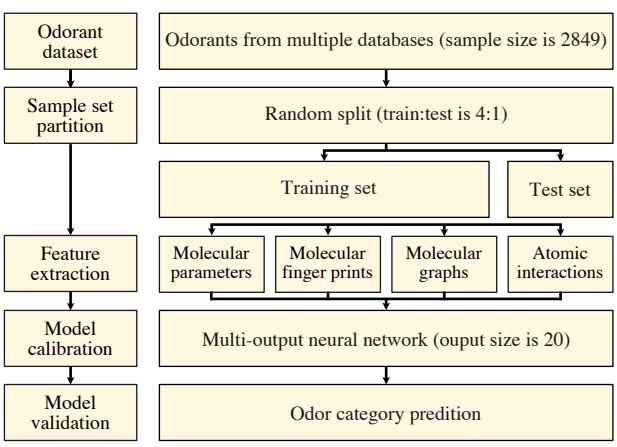

Figure 1: Data processing for calibration and validation of an odor category prediction model.

2.3. Molecular graphic feature extraction

CNNs are highly successful graphic feature extractors, and are commonly developed with high accuracy by large training datasets [38]. Given the utility of convolution kernels and DNNs, CNNs have played a critical role in image and video processing [39]. Recently, molecular graph embedding has been used to model the relationships between chemical compounds [31]. To investigate the feasibility of molecular graphic presentation for odor category prediction, we used 4 types of effective CNNs, including the VGG-16, Restnet, Densnet, and Alexnet, as feature extractors for generating embedding from molecular images in the present study (Fig. 2a). Detailed structures for these CNNs have been previously presented [40–43]. In the present study, we used pre-trained CNN models for odor category prediction to overcome the limitation of sample size.

2.4. Molecular sequence feature extraction

As an end-to-end supervised learning algorithm, graph neural networks (GNNs) have been widely applied for sequence embedding in various fields [44]. Given that odorants can be described as molecular topology graphs using SMILES, we considered GNNs to be appropriate for molecular presentation. Broadly speaking, graph transformers are considered to be a powerful tool for handling molecular presentation through encoding via SMILES, which has been used to predict compound protein interactions, virtual screening, and molecular parameters [45].

Although the molecular graph transformer neural network (MGTNN) has strong potential for molecular modeling, deep learning models always require a large amount of labeled data for training [46]. To overcome the above problems, we used a self-supervised graph transformer (GROVER) to obtain presentation information from the odorants for odor category prediction. A briefly description of the GROVER is given in Fig. 2b. The pre-training architecture was mainly composed of two parts: i) a transformer-based neural network, and ii) a GNN for molecular structure extraction [46]. The input of the model was an odorant graph presentation $\mathcal{G} = (V, E)$, where V was the set of atoms and E was the set of bonds. Specifically, $v_i \in V$ and $e_{i,j} \in E$ were the i-th atom and bond between the i-th and j-th atom, respectively. The GNN was designed to embed extraction according to queries ($\boldsymbol{Q}$), keys ($\boldsymbol{K}$), and values ($\boldsymbol{V}$) from the atoms in molecular graphs ($\mathcal{G}$). The message transmission process of the GNN, as well as the neighborhood aggression between an atom (v) and its neighbors ($\mathcal{N}_v$) in an odorant ($\mathcal{G}$), were adopted to iteratively (L) update hidden states ($\boldsymbol{h}_v$) for atom v, which can be written as:

$$\begin{aligned} \boldsymbol{m}_v^{(l,k)} &= \text{Aggregate}^{(l)}(\{(\boldsymbol{h}_v^{(l,k-1)}, \boldsymbol{h}_u^{(l,k-1)}, \boldsymbol{e}_{v,u}) | u \in \mathcal{N}_v\}) \\ \boldsymbol{h}_v^{(l,k)} &= \sigma(\boldsymbol{W}^l \boldsymbol{m}_v^{(l,k)} + \boldsymbol{b}^{(l)}) \\ \boldsymbol{h}_{\mathcal{G}} &= \text{Readout}(\{\boldsymbol{h}_v^{(0,K_0)}, \ldots, \boldsymbol{h}_v^{(L,K_L)} | v \in V\}) \end{aligned} \tag{2}$$

where $\boldsymbol{m}_v^{(l,k)}$ indicates the passing message for atom v under the k-th step of the l-th iteration. Here, we suppose each iteration (l) contains K_l steps. $\text{Aggregate}^{(l)}(\cdot)$ is an aggregation function, which can be selected from the mean, max pooling, or graph attention mechanism. $\sigma(\cdot)$ is the activation function, and $\boldsymbol{h}_{\mathcal{G}}$ is the graph-level representation generated by a Readout operation. The resulting matrices ($\boldsymbol{Q}, \boldsymbol{K}, \boldsymbol{V}$) were fed to the transformer module, which was composed of graph multi-head attention blocks:

$$\begin{aligned} \text{MultiHead}(\boldsymbol{Q}, \boldsymbol{K}, \boldsymbol{V}) &= \text{concat}(\text{head}_1, \text{head}_2, \ldots, \text{head}_k)\boldsymbol{W}^O \\ \text{head}_i &= \text{Attention}(\boldsymbol{Q}\boldsymbol{W}_i^Q, \boldsymbol{K}\boldsymbol{W}_i^K, \boldsymbol{V}\boldsymbol{W}_i^V) \\ \text{Attention}(\boldsymbol{Q}, \boldsymbol{K}, \boldsymbol{V}) &= \text{softmax}(\boldsymbol{Q}\boldsymbol{K}^T/\sqrt{d})\boldsymbol{V} \end{aligned}$$

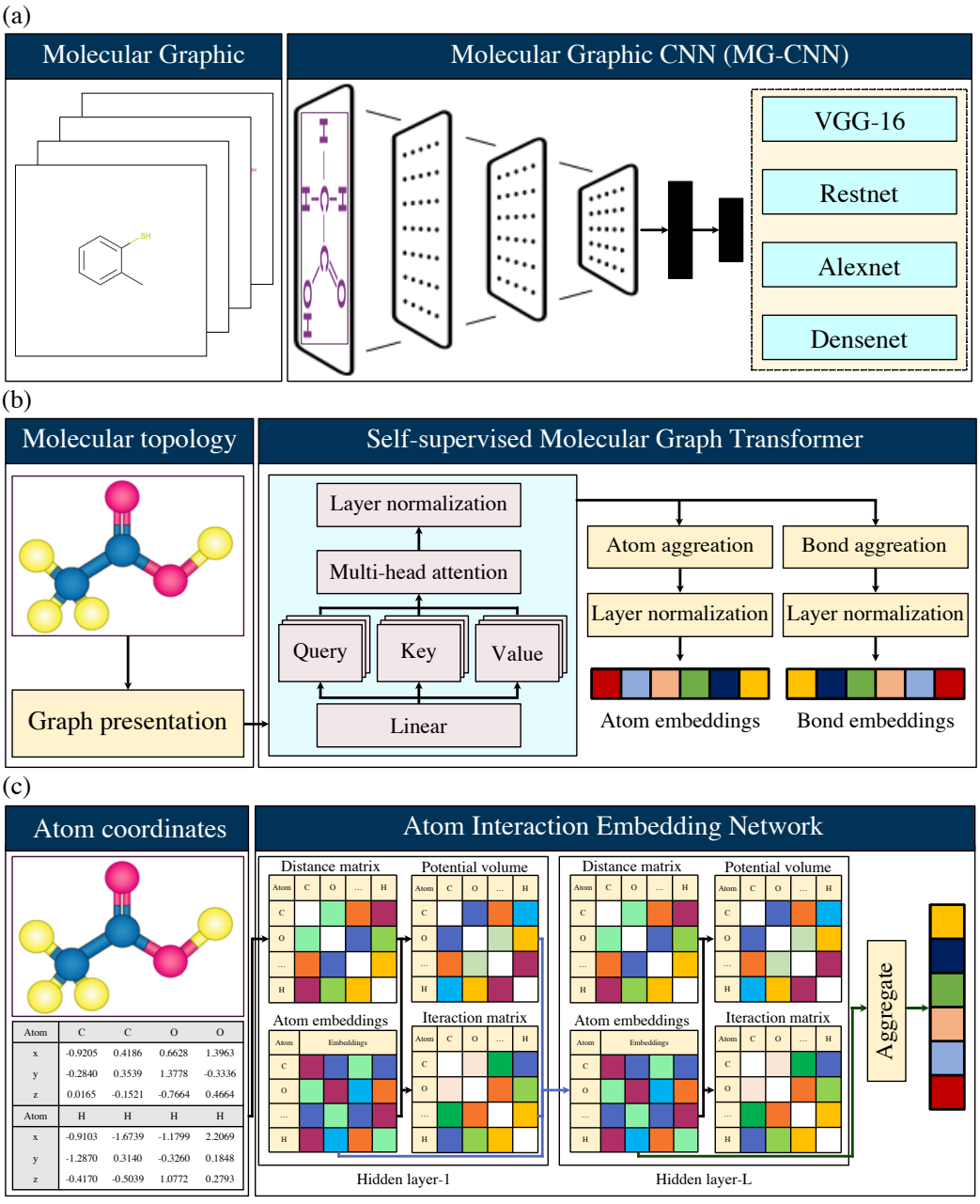

Figure 2: Overview of the design of molecular feature extractors, including (**a**) a molecular graphic convolution neural network (MG-CNN), (**b**) molecular graph transformer neural network (MGT-NN), and (**c**) atom interaction neural network (AINN).

(3)

where $\boldsymbol{W}_i^{\boldsymbol{Q}}$, $\boldsymbol{W}_i^{\boldsymbol{K}}$, $\boldsymbol{W}_i^{\boldsymbol{V}}$ are the projection matrices of head$_i$. d indicates the dimension of $\boldsymbol{q}$ and $\boldsymbol{k}$.

The self-supervised learning tasks in the present study were assigned as contextual property prediction, and graph-level motifs, as well as molecular components, were used to predict links between both nodes and edges. In summary, we employed a pre-trained model, calibrated with 10 million molecules, as a molecular topology feature extractor in the present study. Instances of atom embedding (2048 dimensions) and bond embedding (2048 dimensions) generated by the above-mentioned procedure were used for odor category prediction. This simple strategy has been demonstrated to be a powerful method in terms of graph expression and structure information extraction [47]. Details regarding graph transformers can be found elsewhere [48].

2.5. Atomic interaction embedding

Numerous studies have confirmed that atom interactions are crucial to odor perception [49, 50]. Consequently, molecular features generated by atomic interactions may be feasible for odor category prediction. In the present study, we modeled interactions between atoms in an odorant molecule using a DNN-based model as a molecular feature extractor. A brief description of the process for the AINN is given

in Fig. 2c. Formally, given an odorant $\mathcal{O} = \{(a_i, \boldsymbol{c}_i)\}_{i=1}^{\mathcal{N}_{atom}}$, where a_i is the i-th atom type, $\boldsymbol{c}_i \in \mathbb{R}^2 or \mathbb{R}^3$ is the coordinate vector of the i-th atom, and N_{atom} is the total number of atoms for the odorant. To obtain an atom embedding description for the odorant, $\mathcal{V}_{\mathcal{O}} = \{(\boldsymbol{v}_i, \boldsymbol{c}_i)\}_{i=1}^{\mathcal{N}_{atom}}$, where $\boldsymbol{v}_i \in \mathbb{R}^d$ is the embedded vector for the i-th atom. The embedding dimensionality d is a hyper-parameter that must be assigned before training, and these atom embeddings were initialized randomly and optimized via back propagation. To select the update strategy for the above-mentioned embeddings, we referred to the previous use of DNNs with common graph-structured datasets [51, 52]. Accordingly, the atom embeddings were updated as follows:

$$\begin{aligned} \boldsymbol{v}_i^{(l+1)} &= f(\boldsymbol{v}_i^l) + \sum_{j \in \mathcal{O} \setminus i} g(\boldsymbol{v}_j^{(l)}, P_{i,j}^{(l)}, \alpha_{i,j}^{(l)}) \\ P_{i,j}^{(l)} &= f(\boldsymbol{v}_i^{(l)}, \boldsymbol{v}_j^{(l)}, dist_{i,j}) \\ \alpha_{i,j}^{(l)} &= f(\boldsymbol{v}_i^{(l)}, \boldsymbol{v}_j^{(l)}, dist_{i,j}) \\ dist_{i,j} &= ||\boldsymbol{c}_i - \boldsymbol{c}_j|| \end{aligned} \tag{4}$$

where $f(\cdot)$ and $g(\cdot)$ were the neural networks. $P_{i,j}^{(l)} \in \mathbb{R}$ and $\alpha_{i,j}^{(l)} \in \mathbb{R}$ indicate the potential volume and interaction factor between the i-th and j-th atoms at the l-th hidden layer, respectively. $dist_{i,j} \in \mathbb{R}$ was the Euclidean distance between the i-th and j-th atoms. Thus, the atom interaction embeddings for the odorant ($\boldsymbol{x}_{\mathcal{O}} \in \mathbb{R}^d$) could be calculated by:

$$\boldsymbol{x}_{\mathcal{O}} = \text{Aggregate}(\{\boldsymbol{v}_i\}_{i=1}^{\mathcal{N}_{atom}}) \tag{5}$$

where Aggregate$(\cdot)$ was the aggregate function, which was mean pooling in the present study. As an option, we added a residual part to prevent the vanishing gradient problem in the DNN (res-AINN), which could be defined as follows:

$$\boldsymbol{v}_i^{(l+1)} = Norm(f(\boldsymbol{v}_i^l) + \sum_{j \in \mathcal{O} \setminus i} g(\boldsymbol{v}_j^{(l)}, P_{i,j}^{(l)}, \alpha_{i,j}^{(l)}) + \boldsymbol{v}_i^l) \tag{6}$$

Finally, the odorant embeddings $\boldsymbol{X}_{\mathcal{O}} = \{\boldsymbol{x}_{\mathcal{O}_i}\}_{i=1}^{\mathcal{N}_{sample}}$ were selected as inputs for subsequent models. In this study, the hyper-parameters L, dimensions of embeddings d, learning rate η, and learning epochs were selected as 6, {32, 64, 128, 256, 512, 1024}, 0.001, and 200, respectively. We considered the feasibility of using molecular 2D and 3D coordinates, and discussed the embedding results. Detailed information regarding atom interaction embedding can be found in other publications [29].

3. Results and discussion

3.1. Data analysis

We employed five different molecular structure representations, including odorant molecular parameters (MP), molecular fingerprints (FP), pre-trained molecular graphic embeddings, pre-trained molecular graph transformer embeddings, and atom interaction embeddings in the present study. First, we visualized the numeric vectors in low-dimensional space using Barnes-Hut t-distributed stochastic neighbor embedding (t-SNE) as an unsupervised statistical method. This method has been widely applied for high-dimensional data visualization [53]. The t-SNE presentation of the odorants based on the above-mentioned vectors is illustrated in Fig. 3 and Fig. S1. As reported in previous studies, each odorant contained multi-odor category labels [15, 16, 26, 28, 30]. Therefore, the distribution of odor categories was visualized using colors representing alpha values. Molecular graphic features extracted by Restnet (Fig. 3c) produced a better result than other molecular features because most odorants from the same odor category are clustered together. In contrast, odor cluster overlapping was observed more frequently in the t-SNE map generated from molecular fingerprints (Fig. 3a), molecular parameters (Fig. 3b), and molecular graph transformers (Fig. 3d). Molecular graphs generated from four combined types of pre-trained CNNs produced competitive results compared with other molecular descriptors (Fig. S1). This result demonstrates that odor categories are likely to be more strongly related to molecular graphs than other descriptors. Therefore, we inferred that an odor category identification model based on molecular graphic features would be superior.

3.2. Molecular graphic CNN-based feature analysis

Fig. 4 and Table S2 summarize the performance metrics of the odor category identification model based on molecular graphic feature extraction. The details of model calibration, including the optimal epochs, training loss, and elapsed time, are illustrated in Table 1 and Fig. S2. The pre-trained RestNet with DNNs (6 hidden layers) performed significantly better than the other models, with the highest AUC (0.877±0.028, p<0.001) and F1 score (0.725±0.0278, p<0.001) on the test sets. It was followed by the DenseNet (4 hidden layers, AUC 0.876±0.029, F1 score 0.716±0.035), VGG (6 hidden layers, AUC 0.875±0.028, F1 score 0.716±0.033), and AlexNet (5 hidden layers, AUC 0.873±0.029, F1 score 0.723±0.033). The deep residual framework of the most successful model may have overcome the degradation problem that affects deep networks [42]. In addition, the number of hidden layers in the DNN did not play a necessary role in tuning the pre-trained CNN model. To verify the abilities of the models for transfer learning, we compared the prediction performances of the CNNs depending on whether they were pre-trained. These results are illustrated in Fig. 4. We found that the pre-trained models had significantly (p<0.001) higher accuracy compared with the models with un-trained CNNs. This indicates that CNNs could learn universal image feature extractors through training with a large dataset (ImageNet). This conclusion is supported by previous research [54].

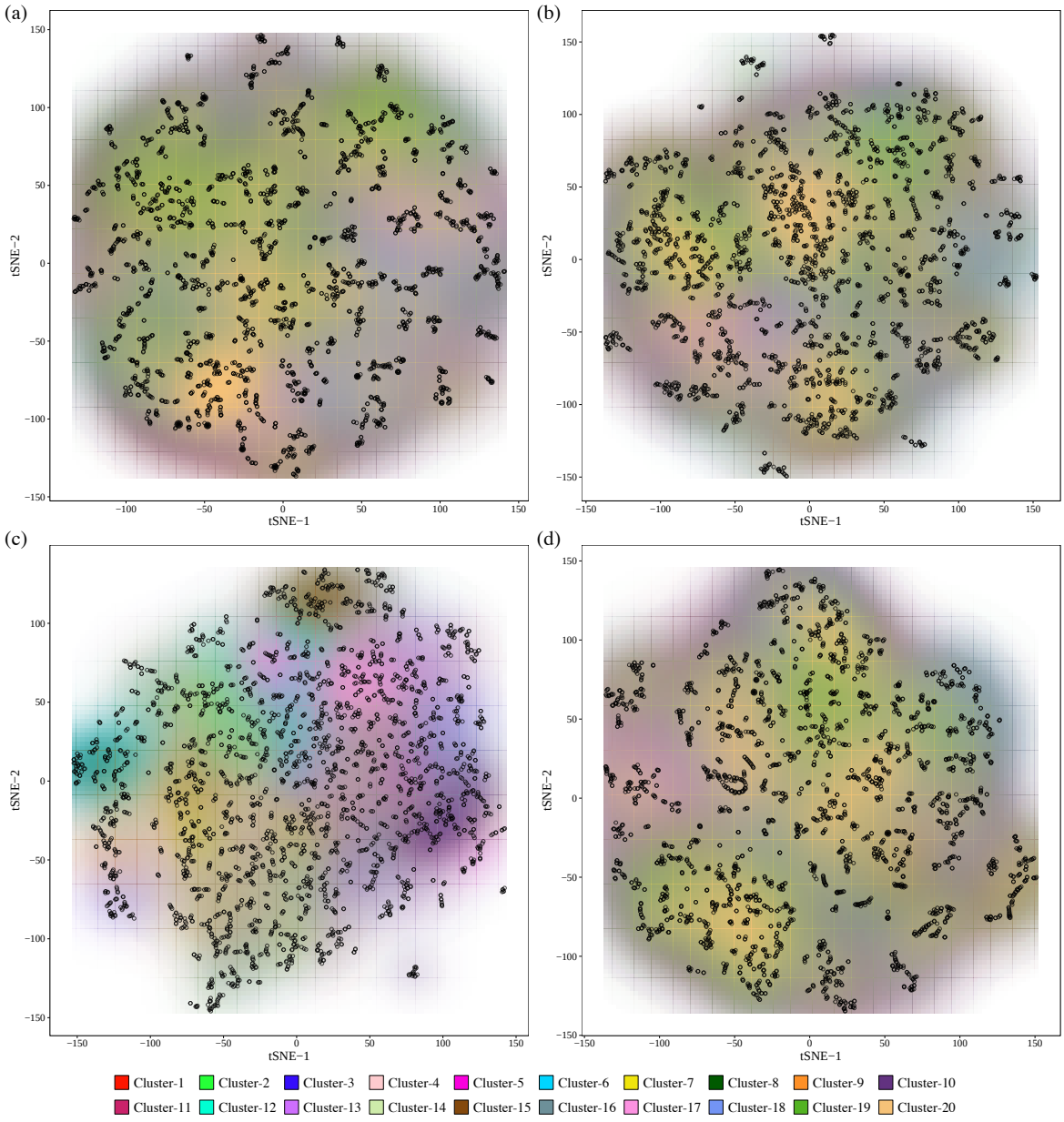

Figure 3: Odorant clustering using Barnes-Hut t-distributed stochastic neighbor embedding (t-SNE) based on (**a**) molecular fingerprints, (**b**) molecular parameters, and (**c**) molecular graphic features extracted via a pre-trained Restnet and (**d**) molecular graph transformer method based on the links between atoms and bonds. tSNE-1 and tSNE-2 were calculated using the t-SNE method. Each point indicates an odorant, colored according to its odor category labels, and the distributions of odor categories are given by the alpha values corresponding to the colors.

3.3. Molecular graph transformer based feature analysis

A summary of the identification accuracy of the MGTNN models is given in Fig. 5 and Table S3. The optimal training epoch, loss, and elapsed time for the MGTNN models are presented in Table 1 and Fig. S3. When the selected atom and bond embeddings were included with 7 hidden layers, the MGTNN model had the highest AUC (0.813±0.035) and F1 score (0.696±0.032) in the test set. In addition, the AUC values for the models independently trained via atom or bond embeddings were 0.812±0.031 and 0.810±0.030, respectively. However, the data were not sufficient to conclude that considering atoms and bonds together produced a significantly more accurate result than when they were included individually ($p>0.001$).

3.4. Atom interaction-based feature analysis

Fig. 6 and Table S4 compares odor sensory category identification according to the molecular features extracted by AINNs. The results indicated that the AINN-DNN model (2D, 512 embedded dimensions) had the highest identification performance in terms of the AUC and F1 score, which

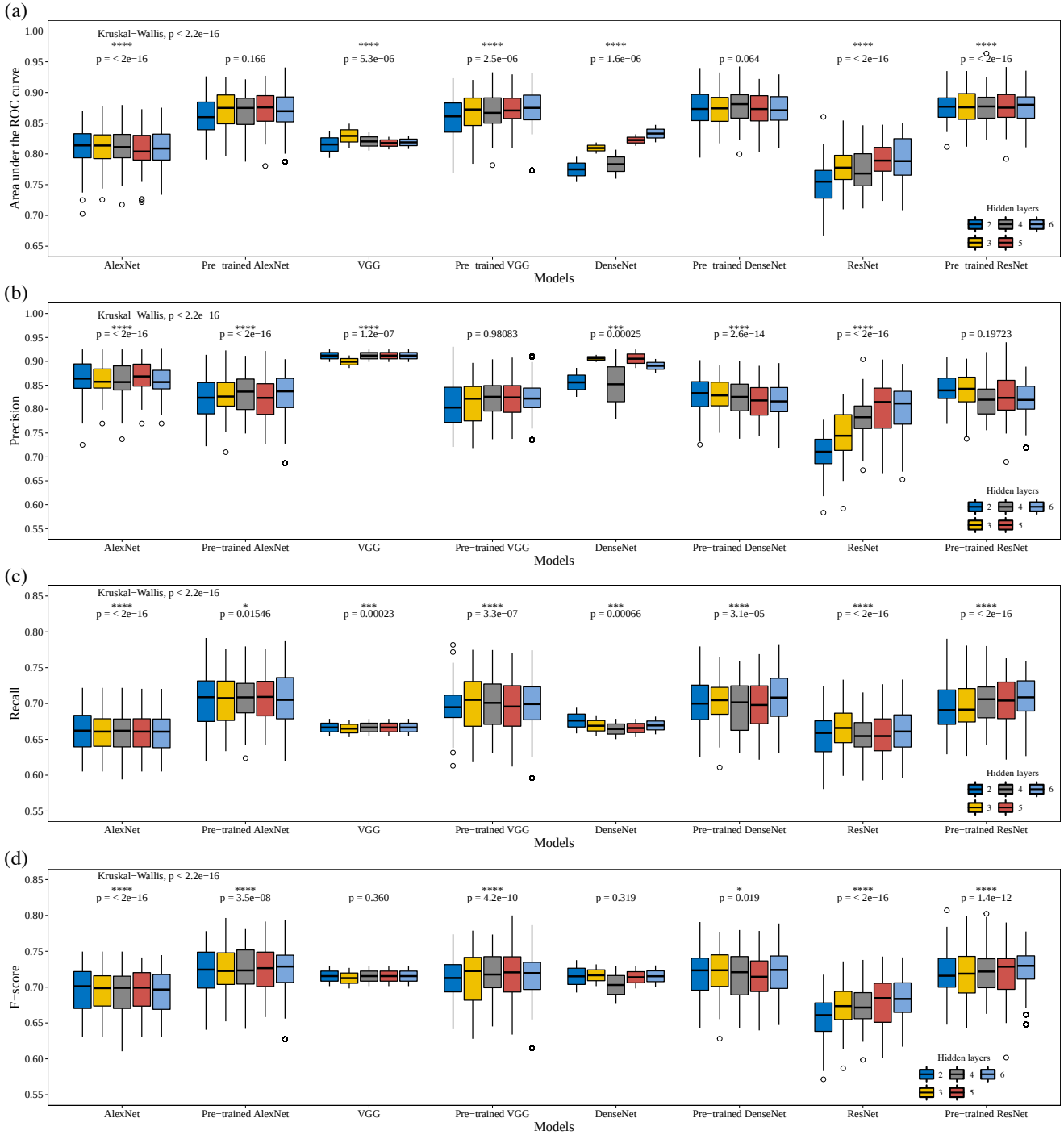

Figure 4: Identification performance of four molecular graphic convolution neural network (MG-CNN) models: AlexNet, VGG, DenseNet, and ResNet. The models were evaluated according to the average identification AUC (**a**), precision (**b**), recall (**c**), and F1 score (**d**). Results were evaluated using the nonparametric Wilcoxon signed-rank test.

were 0.807±0.035 ($p<0.01$) and 0.696±0.023, respectively. However, we cannot claim that the molecular 2D coordinates were better for identification than the 3D coordinates because the analyses for both had a high p-value. Furthermore, the models with residual modules did not exhibit a significant increase, likely because the vanishing gradient is not the critical obstacle limiting AINN performance. In addition, the dimension of atom embedding vectors did not have a significant effect on the accuracy of odor category identification. The optimal training epoch, loss, and elapsed time for AINN models are listed in Table 1 and Fig. S4. We found that the modeling time for 2D coordinates was significantly smaller than that for 3D coordinates ($p<0.001$).

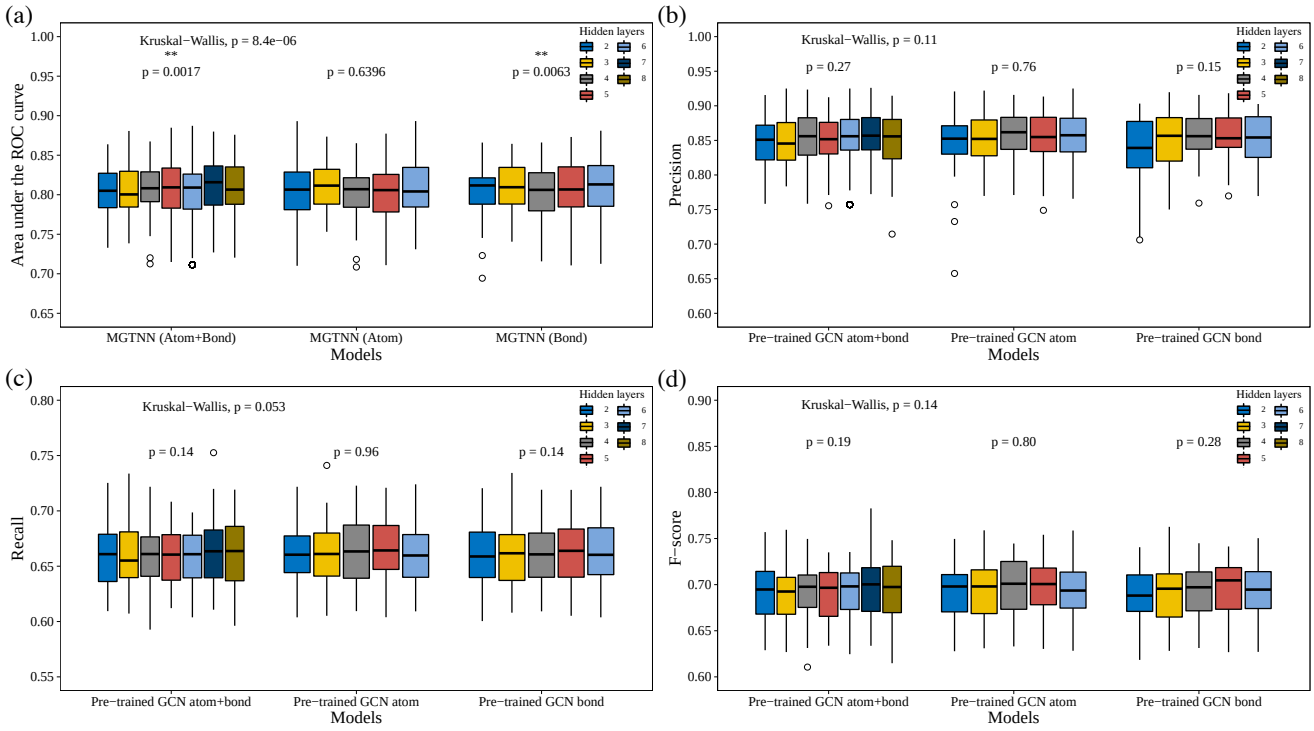

Figure 5: Determination of odor category by molecular graph transformer neural network (MGTNN) models for atom embeddings only, bond embeddings only, and combinations thereof. Models were evaluated according to the average identification AUC (**a**), precision (**b**), recall (**c**), and F1 score (**d**). Results were subjected to the nonparametric Wilcoxon signed-rank test.

This suggests that the presented AINN models do not need spatial embedding for odor sensory identification.

3.5. Performance comparison

To identify the model with the best comprehensive performance for odor category identification, we compared the five types of models in terms of performance metrics, as presented in Fig. 7 and Table 2. Table 1 and Fig. S5 illustrates the optimal training epoch, loss, and elapsed time for the above-mentioned models. The predicted accuracies for each odor sensory category are summarized in Fig. S6-S10. The results confirmed that the model trained using molecular graphic features extracted via a pre-trained ResNet had significantly better performance than the other models (AUC 0.877±0.028, F1 score 0.726±0.028, $p<0.0001$), followed by the AINN-DNN (AUC 0.807±0.035, F1 score 0.696±0.030), MPs (AUC 0.806±0.033, F1 score 0.689±0.031), MGTNN (AUC 0.804±0.028, F1 score 0.692±0.029), and FPs (AUC 0.796±0.036, F1 score 0.688±0.033). This ranking could likely be explained by the high correlation between the olfactory sensory information and the molecular graphic features of the odorants compared with the other molecular descriptors. We found that the AINN-DNN model had the highest precision (0.861±0.038, $p<0.0001$). We confirmed that that although more epochs were needed to train the ResNet models, the training time was shorter than that for the AINN-DNN and MGTNN models. The fast convergence speed could contribute to the transfer-learning mechanism. Although the number of parameters was abundant for the ResNet model, we did not train these parameters, but instead used those from the pre-trained models. The pre-trained models could overcome the limitation of insufficient samples for training DNN models. A similar conclusion was found previously [55]. In summary, we suggest that an end-to-end DNN with molecular graphic features extracted via a pre-trained ResNet is an optimal model for predicting the sensory categories of odorants.

3.6. Discussion

The accurate and effective prediction of odor sensory categories is vital for developing machine-learning-based GC/O. To develop an olfaction-based sensory system, we need not only bio-sensors to encode odorants (odor receptor imitation), but also a brain-like odor signal decoding algorithm. Although many studies have examined SORs, most have focused on predicting ODs [15, 16, 18, 21, 31]. Even though most ODs can be predicted, infrequent ODs were difficult to be identified. For excample, Snitz proposed a mostly perfect result in prediciting 64 smell percepts with 100 % precision and 102 smells with 90.35 %, but infrequent smells, such as almond, apricot and chocolate, had been found to have poor prediction performance [16]. This could be explained by the extreme imbalance in the data distribution, as well as the insufficient number of training samples. Unlike the above-mentioned studies, we want to find useful odorant structure features for odor sensory categories indentification.

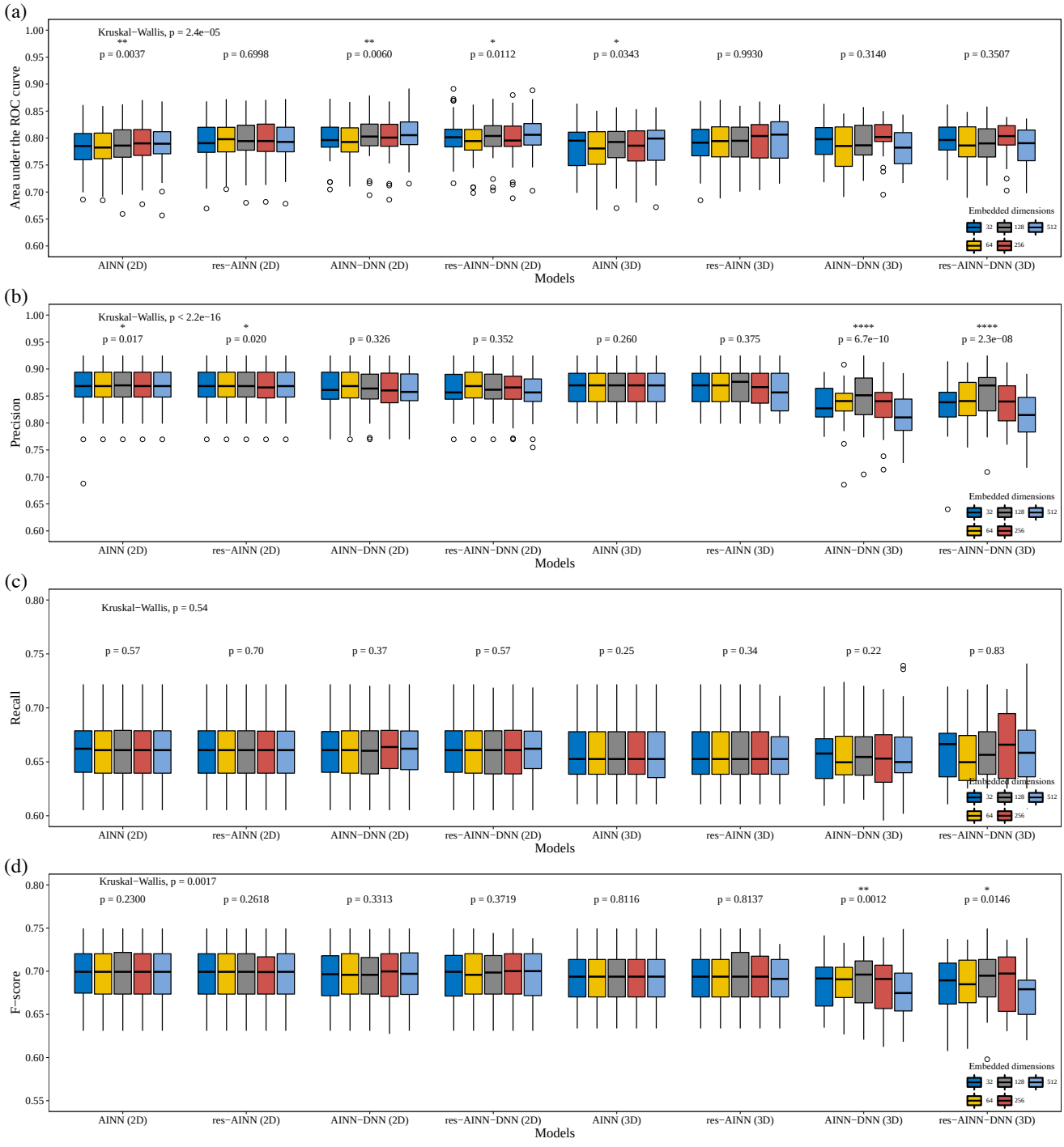

Figure 6: Results for odor category determined by atom interaction neural network (AINN) models. The models were evaluated according to the average identification area under the curve (AUC) (**a**), precision (**b**), recall (**c**), and F1 score (**d**). The data were subjected to a nonparametric Wilcoxon signed-rank test.

Table 1
Modeling and training parameters for DNN models calibration.

Model name	Input dimension	Hidden layers	Training epoch	Loss	Elapsed time (s)
FP-based	2048	6	83±42.3	0.00891±0.000942	32.5±16.6
MP-based	1000	6	91.8±46.1	0.00975±0.000528	36±18
MG-CNN-based	512	6	128±42.6	0.00672±0.000803	51.7±17.3
MGT-NN-based	4096	7	105±49.9	0.0100±0.000469	74.2±42.3
AINN-based	512	6	59±25.2	0.0107±0.000622	117±53.4

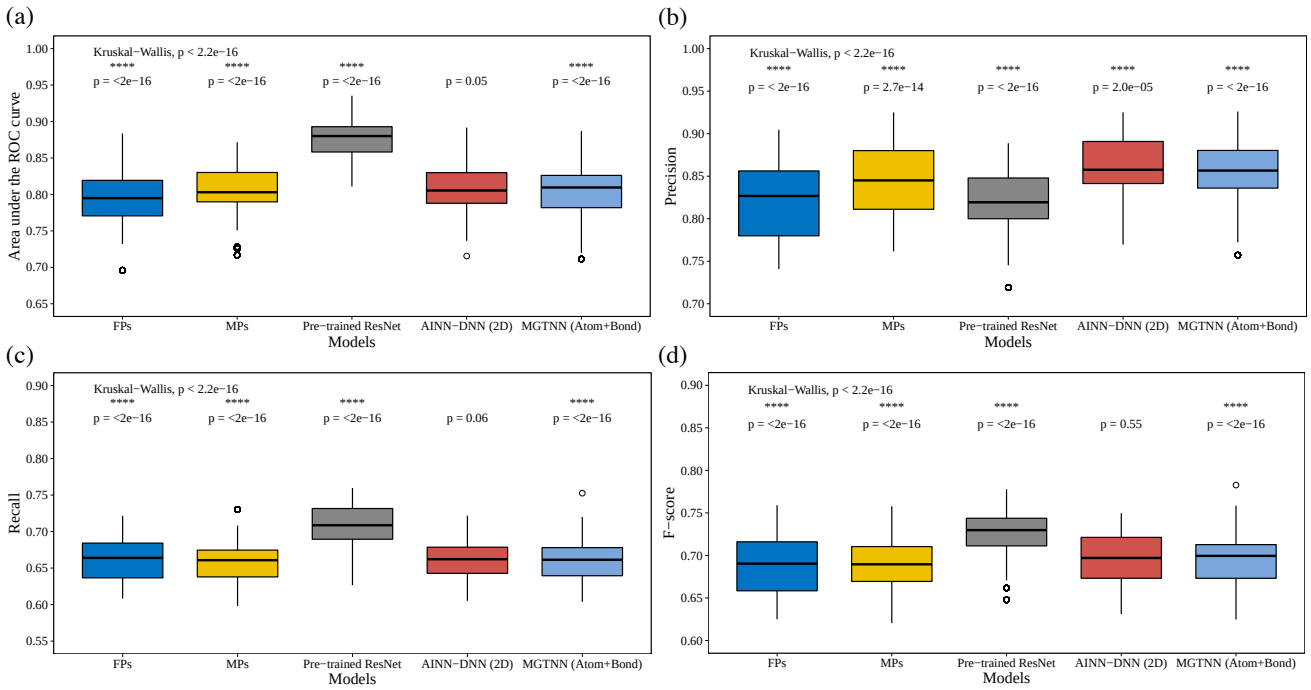

Figure 7: Identification accuracies of DNN models using molecular features extracted via FP-, MP-, MG-CNN-, MGTNN-, and AINN-based DNN models. The data were evaluated using the nonparametric Wilcoxon signed-rank test.

Table 2
Odor sensory category identification accuracy comparison of DNN models using multi-type of odorant structure features.

Model name	AUC-ROC	Precision	Recall	F1 score
FP-based	0.796±0.036	0.82±0.046	0.662±0.029	0.688±0.033
MP-based	0.806±0.033	0.843±0.039	0.658±0.028	0.689±0.031
MG-CNN-based	0.877±0.028	0.822±0.037	0.71±0.028	0.726±0.028
MGT-NN-based	0.804±0.036	0.855±0.036	0.659±0.025	0.692±0.029
AINN-based	0.807±0.035	0.861±0.038	0.662±0.027	0.696±0.030

Here, we focused on establishing relationships between molecular features and odor sensory categories via an end-to-end learning strategy, which is expected to play a decoding role in bio-olfaction. The MPs and FPs in the present study had poor performance, indicating that focusing solely on physiology-chemical parameters could result in the loss of some critical information related to olfaction. In contrast to relying on tabular features, molecular graph CNNs-based features would be more appropriate for learning useful odor sensory expression. We also considered a transfer learning strategy for dealing with the problem of insufficient training samples. Our results confirm that pre-trained CNNs, combined with a 'vanilla' DNN, can effectively establish relationships between molecular features and odor sensory categories. Furthermore, our data suggest that molecular graphic features are optimal for describing odorant protein interactions according to human olfaction. Existing GC/O methods have focused on just 8 ODs in one olfaction sensory evaluation task, as limited by the odor memory of the assessors [56–58]. Odor analysis precision is also limited by their odor memory. Therefore, the proposed model can apply a reliable references for human panlists to reduce trainning cost.

This study has several limitations. First, more attention should be focused on atom interaction-based embeddings, although the AINN in the present study had poor performance. Biological studies have indicated that atom interactions play a critical role in mammal olfaction [59–61]. The poor accuracy of the AINN was likely caused by insufficient odorants and an inappropriate modeling approach. Moreover, we did not consider the electronic interactions between atoms, which may be suitable for olfaction sensory encoding. Self-supervised strategies combined with proper modeling techniques and trained with abundant molecules merit further investigation. Furthermore, synergism, odor neutralization and the predicatable of a fragrance mixture has still not been quantified [62–64]. In present study, we focus on single odor molecule smell perception prediction, which is not appropriate for modeling odor synergism and neutralization. For fragrance mixture prediction, mass spectral would be feasible for model calibration. In the future, we plan to attempt to improve our framework for molecular

structure feature extraction using other algorithms, and to try to explore the feasibility of metric modeling using Riemannian manifolds, such as the Grassmann or symmetric positive definite manifold [65, 66]. We expect that it will be difficult to find a reasonable algorithm when performing metric learning in Riemannian space. However, this is an interesting problem for future investigation. In addtion, data fusion would also be an effective strategy for increasing the accurcay of odor category identification models.

4. Conclusions

The SOR by DNNs via the structure features of odorants has attracted great attention during the past decade. Due to the limited knowledge on binding mechanism between odorant molecules and olfactory receptors, however, it is not sure what kind of structural features play the most important role in smell recognition. Here, we utilized a DNN-based multi-label classifier for odor sensory category identification using various molecular features. Specifically, we examined the possibility of predicting odor categories based on molecular parameters, fingerprints, and graphics, as well as graph attention network embedding and atom interactions. Our results indicated that molecular 2D graphic data were strongly related to sensory information about olfaction. Extensive experiments confirmed that a 'vanilla' DNN with molecular graphic features, extracted via ResNet, was optimal for odor perception category identification. We anticipate that transfer learning is a viable and powerful technique for modeling the relationships between molecular structures and odor perception categories. Our proposed approach could be applied in the development of AI-based odor sensors. We believe that this study is among the first to examine the importance of molecular graphic features when establishing relational models between molecular structures and odor sensory categories. Our approach may not only serve as a realistic solution for introducing AI into olfactometry, but may also offer a novel perspective for investigating the mechanisms of human olfaction.

Declaration of competing interest

The authors declare that they have no known competing financial interests or personal relationships that could have appeared to influence the work reported in this paper.

CRediT authorship contribution statement

Liang Shang: Conceptualization, Methodology, Experiment, Writing. **Chuanjun Liu:** Conceptualization, Method, Supervision, Reviewing. **Fengzhen Tang:** Supervision, Reviewing. **Bin Chen:** Supervision, Reviewing. **Lianqing Liu:** Reviewing. **Kenshi Hayashi:** Reviewing.

Acknowledgements

This research was supported by China Postdoctoral Science Foundation (2021M703399), the National Key Research and Development Program of China (No. 2020YFB13400), National Nature Science Foundation of China (No. 61803369 and 61801400), and JSPS KAKENHI Grant (No. 18H03782).

Appendix A. Supplementary data

Supplementary data associated with this article can be found, in the online version, at http://dx.doi.org/.

References

[1] A. Maurya, J. Prasad, S. Das, A. K. Dwivedy, Essential oils and their application in food safety, Front. Sustain. Food Syst. 5 (2021).

[2] T. E. Acree, GC/Olfactometry GC with a sense of smell, Anal. Chem. 69 (1997) 170A–175A.

[3] S.-T. Chin, P. J. Marriott, Review of the role and methodology of high resolution approaches in aroma analysis, Anal. Chim. Acta. 854 (2015) 1–12.

[4] A.-S. Barwich, What makes a discovery successful? the story of linda buck and the olfactory receptors, Cell 181 (2020) 749–753.

[5] K. Mori, Y. K. Takahashi, K. M. Igarashi, M. Yamaguchi, Maps of odorant molecular features in the mammalian olfactory bulb, Physiol. Rev. 86 (2006) 409–433.

[6] B. Auffarth, Understanding smell-the olfactory stimulus problem, Neurosci. Biobehav. Rev. 37 (2013) 1667–1679.

[7] R. Haddad, H. Lapid, D. Harel, N. Sobel, Measuring smells, Curr. Opin. Neurobiol. 18 (2008) 438–444.

[8] C. Liu, H. Miyauchi, K. Hayashi, Deepsniffer: A meta-learning-based chemiresistive odor sensor for recognition and classification of aroma oils, Sens. Actuators B Chem. 351 (2022) 130960.

[9] L. B. Ayres, F. J. V. Gomez, J. R. Linton, M. F. Silva, C. D. Garcia, Taking the leap between analytical chemistry and artificial intelligence: A tutorial review, Anal. Chim. Acta. 1161 (2021) 338403.

[10] R. Chacko, D. Jain, M. Patwardhan, A. Puri, S. Karande, B. Rai, Data based predictive models for odor perception, Sci. Rep. 10 (2020) 17136.

[11] L. Shang, C. Liu, Y. Tomiura, K. Hayashi, Artificial odor cluster map of odorant molecular parameters and odor maps in rat olfactory bulbs, Chem. Senses 41 (2016) E212. 17th International Symposium on Olfaction and Taste (ISOT), Yokohama, JAPAN, JUN 05-09, 2016.

[12] Y. Nozaki, T. Nakamoto, Predictive modeling for odor character of a chemical using machine learning combined with natural language processing, PLoS ONE 13 (2018) e0208962.

[13] H. Zhang, P. Ma, J. Shu, B. Yang, J. Huang, Rapid detection of taste and odor compounds in water using the newly invented chemi-ionization technique coupled with time-of-flight mass spectrometry, Anal. Chim. Acta 1035 (2018) 119–128.

[14] K. Snitz, O. Perl, D. Honigstein, L. Secundo, A. Ravia, A. Yablonka, Y. Endevelt-Shapira, N. Sobel, Smellspace: An odor-based social network as a platform for collecting olfactory perceptual data, Chem. Senses 44 (2019) 267–278.

[15] R. Kumar, R. Kaur, B. Auffarth, A. P. Bhondekar, Understanding the odour spaces: A step towards solving olfactory stimulus-percept problem, PLoS ONE 10 (2015) e0141263.

[16] K. Snitz, A. Yablonka, T. Weiss, I. Frumin, R. M. Khan, N. Sobel, Predicting odor perceptual similarity from odor structure, PLoS Comput. Biol. 9 (2013) e1003184.

[17] C. Liu, L. Shang, K. Hayashi, Co-occurrence-based clustering of odor descriptors for predicting structure-odor relationship, in: IEEE International Symposium on Olfaction and Electronic Nose (ISOEN), pp. 1–4.

[18] J. Loetsch, D. Kringel, T. Hummel, Machine learning in human olfactory research, Chem. Senses 44 (2019) 11–22.

[19] E. Esme, M. S. Kiran, The performance analysis of extreme learning machines on odour recognition, in: Proceedings of the 2018 2nd International Conference on Cloud and Big Data Computing, ICCBDC 18, Association for Computing Machinery, New York, NY, USA, 2018, pp. 87–92.

[20] Y. Choi, K. Kim, S. Kim, D. Kim, Identification of odor emission sources in urban areas using machine learning-based classification models, Atmos 13 (2022) 100156.

[21] T. Debnath, T. Nakamoto, Predicting human odor perception represented by continuous values from mass spectra of essential oils resembling chemical mixtures, PLoS ONE 15 (2020) e0234688.

[22] D. Hasebe, T. Nakamoto, A model to predict mass spectrum from odor impression using deep neural network, in: 2021 IEEE Sensors, pp. 1–4.

[23] V. Hamedpour, P. Oliveri, R. Leardi, D. Citterio, Chemometric challenges in development of paper-based analytical devices: Optimization and image processing, Anal. Chim. Acta 1101 (2020) 1–8.

[24] Q. Liu, D. Luo, T. Wen, H. GholamHosseini, X. Qiu, J. Li, POI-3DGCN: Predicting odor intensity of monomer flavors based on three-dimensionally embedded graph convolutional network, Expert Syst. Appl. (2022) 116997.

[25] E. D. Gutiérrez, A. Dhurandhar, A. Keller, P. Meyer, G. A. Cecchi, Predicting natural language descriptions of mono-molecular odorants, Nat. Commun. 9 (2018) 4979.

[26] L. Shang, C. J. Liu, Y. Tomiura, K. Hayashi, Machine-learning-based olfactometer: Prediction of odor perception from physicochemical features of odorant molecules, Anal. Chem. 89 (2017) 11999–12005.

[27] A. Dravnieks, Odor quality: Semantically generated multidimensional profiles are stable, Science 218 (1982) 799–801.

[28] L. Shang, C. Liu, B. Chen, F. Tang, L. Liu, K. Hayashi, Machine-learning-based olfactometry: Odor descriptor clustering based on bayesian embedding model and its prediction from molecular graphic features, Submitted (2021).

[29] M. Tsubaki, T. Mizoguchi, Fast and accurate molecular property prediction: learning atomic interactions and potentials with neural networks, J. Phys. Chem. 10 (2019) 2066–2067.

[30] B. Sánchez-Lengeling, J. N. Wei, B. K. Lee, R. C. Gerkin, A. Aspuru-Guzik, A. B. Wiltschko, Machine learning for scent: Learning generalizable perceptual representations of small molecules, ArXiv abs/1910.10685 (2019).

[31] A. Sharma, R. Kumar, S. Ranjta, P. K. Varadwaj, SMILES to smell: Decoding the structure-odor relationship of chemical compounds using the deep neural network approach, J. Chem. Inf. Model. 61 (2021) 676–688.

[32] B. A. Johnson, Z. Xu, S. S. Ali, M. Leon, Spatial representations of odorants in olfactory bulbs of rats and mice: SimilaritiesÍ and differences in chemotopic organization, J. Comp. Neurol. 514 (2009) 658–673.

[33] Sigma-Aldrich, Flavors and fragrances products catalog, Merck KGaA: Darmstadt (2016).

[34] H. Arn, T. E. Acree, E. T. Contis, C.-T. Ho, C. J. Mussinan, T. H. Parliment, F. Shahidi, A. M. Spanier, Flavornet: A database of aroma compounds based on odor potency in natural products, in: Developments in Food Science, volume 40, Elsevier, 1998, p. 27.

[35] G. Landrum, Open-source cheminformatics, GitHub and SourceForge 3 (2012).

[36] S. Kim, J. Chen, T. Cheng, A. Gindulyte, J. He, S. He, Q. Li, B. A. Shoemaker, P. A. Thiessen, B. Yu, L. Zaslavsky, J. Zhang, E. E. Bolton, PubChem in 2021: New data content and improved web interfaces, Nucleic Acids Res. 49 (2021) D1388–D1395.

[37] H. Moriwaki, Y.-S. Tian, N. Kawashita, T. Takagi, Mordred: a molecular descriptor calculator, J. Cheminformatics 10 (2018) 4.

[38] J.-L. Wang, H.-N. Wu, T. Huang, M. Xu, Output synchronization in coupled neural networks with and without external disturbances, IEEE Trans. Control. Netw. Syst. 5 (2018) 2049–2061.

[39] T. Zhang, M. Waqas, Z. Liu, S. Tu, Z. Halim, S. U. Rehman, Y. Li, Z. Han, A fusing framework of shortcut convolutional neural networks, Inf. Sci. 579 (2021) 685–699.

[40] A. Krizhevsky, I. Sutskever, G. E. Hinton, Imagenet classification with deep convolutional neural networks, Commun. ACM 60 (2017) 84–90.

[41] G. Huang, Z. Liu, L. Van Der Maaten, K. Q. Weinberger, Densely connected convolutional networks, in: Proceedings of CVPR, pp. 2261–2269.

[42] K. He, X. Zhang, S. Ren, J. Sun, Deep residual learning for image recognition, in: Proceedings of CVPR, pp. 770–778.

[43] K. Simonyan, A. Zisserman, Very deep convolutional networks for large-scale image recognition, in: International Conference on Learning Representations (ICLR).

[44] X. Mei, X. Cai, L. Yang, N. Wang, Graph transformer networks based text representation, Neurocomputing 463 (2021) 91–100.

[45] N. Warikoo, Y.-C. Chang, W.-L. Hsu, LBERT: Lexically aware transformer-based bidirectional encoder representation model for learning universal bio-entity relations, Bioinformatics 37 (2021) 404–412.

[46] Y. Rong, Y. Bian, T. Xu, W. Xie, Y. WEI, W. Huang, J. Huang, Self-supervised graph transformer on large-scale molecular data, in: H. Larochelle, M. Ranzato, R. Hadsell, M. F. Balcan, H. Lin (Eds.), Adv. Neural Inf. Process. Syst., volume 33, Curran Associates, Inc., 2020, pp. 12559–12571.

[47] D. Chen, K. Gao, D. D. Nguyen, X. Chen, Y. Jiang, G.-W. Wei, F. Pan, Algebraic graph-assisted bidirectional transformers for molecular property prediction, Nat. Commun. 12 (2021) 3521.

[48] K. Mao, X. Xiao, T. Xu, Y. Rong, J. Huang, P. Zhao, Molecular graph enhanced transformer for retrosynthesis prediction, Neurocomputing 457 (2021) 193–202.

[49] A. Fjaeldstad, H. M. Fernandes, T. J. Van Hartevelt, C. Gleesborg, A. Møller, T. Ovesen, M. L. Kringelbach, Brain fingerprints of olfaction: a novel structural method for assessing olfactory cortical networks in health and disease, Sci. Rep. 7 (2017) 42534.

[50] A. Fjaeldstad, Testing olfactory function and mapping the structural olfactory networks in the brain, Dan. Med. J. 65 (2018).

[51] M. Tsubaki, K. Tomii, J. Sese, Compound-protein interaction prediction with end-to-end learning of neural networks for graphs and sequences, Bioinformatics 35 (2019) 309–318.

[52] L. Chen, X. Tan, D. Wang, F. Zhong, X. Liu, T. Yang, X. Luo, K. Chen, H. Jiang, M. Zheng, TransformerCPI: Improving compound-protein interaction prediction by sequence-based deep learning with self-attention mechanism and label reversal experiments, Bioinformatics 36 (2020) 4406–4414.

[53] L. Shang, C. J. Liu, Y. Tomiura, K. Hayashi, Odorant clustering based on molecular parameter-feature extraction and imaging analysis of olfactory bulb odor maps, Sens. Actuators B Chem. 255 (2018) 508–518.

[54] C. Liu, P. Liu, W. Zhao, X. Tang, Visual tracking by structurally optimizing pre-trained CNN, IEEE Trans. Circuits. Syst. Video Technol. 30 (2020) 153–3166.

[55] N. Pezzotti, B. P. F. Lelieveldt, L. van der Maaten, T. Hollt, E. Eisemann, A. Vilanova, Approximated and user steerable tSNE for progressive visual analytics, IEEE Trans. Vis. Comput. Graph 23 (2017) 1739–1752.

[56] M. Brattoli, E. Cisternino, P. R. Dambruoso, G. de Gennaro, P. Giungato, A. Mazzone, J. Palmisani, M. Tutino, Gas chromatography analysis with olfactometric detection (GC-O) as a useful methodology for chemical characterization of odorous compounds, Sens. 13 (2013) 16759–16800.

[57] M. Aznar, R. López, J. F. Cacho, V. Ferreira, Identification and quantification of impact odorants of aged red wines from Rioja. GC−Olfactometry, quantitative GC-MS, and odor evaluation of HPLC fractions, J. Agric. Food Chem. 49 (2001) 2924–2929.

[58] K. Vene, S. Seisonen, K. Koppel, E. Leitner, T. Paalme, A method for GC-Olfactometry panel training, Chemosensory Perception 6 (2013) 179–189.

[59] M. Mantel, A. Fournel, I. Staedlé, A. Oelschlägel, J. Carro, R. Dubreuil, C. Herrier, T. Livache, A. Haehner, T. Hummel, J.-M. Roy, M. Bensafi, Using a bio-inspired surface resonance plasmon electronic nose for fundamental research on human olfaction, Sens. Actuators B Chem. 350 (2022) 130846.

[60] N. X. Thai, M. Tonezzer, L. Masera, H. Nguyen, N. V. Duy, N. D. Hoa, Multi gas sensors using one nanomaterial, temperature gradient, and machine learning algorithms for discrimination of gases and their

concentration, Anal. Chim. Acta 1124 (2020) 85–93.

[61] C. Liu, L. Shang, H.-T. Yoshioka, B. Chen, K. Hayashi, Preparation of molecularly imprinted polymer nanobeads for selective sensing of carboxylic acid vapors, Anal. Chim. Acta 1010 (2018) 1–10.

[62] G. Hudon, C. Guy, J. Hermia, Measurement of odor intensity by an electronic nose., J. Air Waste Manag Assoc. 50 (2000) 1750–1578.

[63] L. Yan, J. Liu, S. Jiang, C. Wu, K. Gao, The regular interaction pattern among odorants of the same type and its application in odor intensity assessment., Sensors 17 (2017) 1624.

[64] L. Zhang, H. Mao, Y. Zhuang, L. Wang, L. Liu, Y. Dong, J. Du, W. Xie, Z. Yuan, Odor prediction and aroma mixture design using machine learning model and molecular surface charge density profiles, Chem. Eng. Sci. 245 (2021) 116947.

[65] F. Tang, H. Feng, P. Tino, B. Si, D. Ji, Probabilistic learning vector quantization on manifold of symmetric positive definite matrices, Neural Netw. 142 (2021) 105–118.

[66] T. Matsukawa, T. Okabe, E. Suzuki, Y. Sato, Hierarchical Gaussian descriptors with application to person re-identification, IEEE Trans. Pattern Anal. Mach. Intell. 42 (2020) 2179–2194.